Latin American Journal of Solids and Structures
www.lajss.org

Effects of Key Factors on Hull Girder Ultimate Strength Estimation by Progressive Collapse Calculations

Abstract

The estimation of the ship hull girder ultimate strength under vertical bending moments as close to real behavior is vital both for design stage or seagoing life. The maximum load carrying capacity of ship hulls called ultimate strength depends on a number of factors including the strength of the structural material, initial distortions, dimensions and layout of the structural components, the component discretization (idealization) of hull girder section. In this study, the main target is to evaluate the effects of hull girder section component discretization, initial deflection of plates and residual welding stress and 50% corrosion margin for individual structural components on the ultimate hull girder strength. Within this context, hull girder ultimate strength calculations are carried out for ten benchmark ships' cross sections for validation of HULT developed by authors, firstly. Next, to reflect the effect of diverse key factors, selected ships among ten are analysed for different scenarios using progressive collapse analysis based method HULT and with IACS-CSR formulations. Critical collapse moment values of ten mid-ship cross sections are calculated and shown to agree well with the results of previous studies. As a result, both the accuracy of HULT, as well as the effects of diverse key factors on ultimate strength are shown clearly by case studies.

Keywords

Ultimate Strength, Progressive Collapse, Smith Method, Orthotropic Panel, Component Discretization, Initial Distortions.

Hasan Ölmez [a]
Ertekin Bayraktarkatal [b]

[a] Karadeniz Technical University Trabzon, Turkey, hasanolmez@ktu.edu.tr
[b] İstanbul Technical University İstanbul, Turkey, bayrak@itu.edu.tr

http://dx.doi.org/10.1590/1679-78252509

Received 04.10.2015
In revised form 17.06.2016
Accepted 21.06.2016
Available online 27.06.2016

1 INTRODUCTION

Unlike most land based structures, ships and offshore structures operates in a dynamic and unstable sea environment. For the most part of loads caused by sea conditions and own cargos are much less than the structural capacity of the ship's hull girder. However, these structures must not only be designed according to be capable of withstanding normal loads, but also with extreme sea condition scenarios.

At this point, the ultimate strength theme that show us maximum load carrying capacity of hull girder under bending moment is considered very important in the academic area and classification societies. The structural components that form the ships and offshore structures are exposed to large vertical bending moments and especially compression or tension forces in the longitudinal axis in case of hogging and sagging under bad sea conditions. At this point, the ultimate load carrying capacity of the ship is critical measure. If the vessel exposed to primary loads over this critical value during hogging and sagging actions, the hull girder may collapse like breaking in two or something more catastrophic losses (see Figure 1). During these actions, a ship experiences many types of loads divided into specific categories. The two most critical loads in terms of the overall hull girder strength are static calm water loads and the low frequency dynamic loads caused by waves. These loads produce a distribution of longitudinal bending moments and compression/tension loads. If the bending moment value exceeds the ultimate strength value of the hull girder, the ship can fail due to buckling and progressive collapse of the compressed part (Smith, 1997). In recent years, the practical, fast and reliable estimation of the maximum load carrying capacity (ultimate strength) of the ships just before breaks in two under worst conditions becomes vital. The optimum (accuracy, time, practicality) estimation of these values is depends on how accurate the stress-strain behavior of the structural components are established. Published researches about progressive collapse analysis of hull girder can be classified three categories such as (1) derivation of theoretical methods to estimate progressive collapse or ultimate strength; (2) results from theoretical modelling of sections using FEM approaches and (3) reporting of physical experiments on box girders or ship structures. The well-known and most effective methods using for globally progressive collapse analysis of hull girders by different component types are Smith Method (Smith, 1977) and ISUM by (Ueda and Rashed, 1991).

Figure 1: MOL Comfort - 313 m length container ship broke in two in June 2013 (Vesselfinder.com, 2013).

Earlier works by many researchers from (Caldwell, 1965) to (Paik et al., 2008), from (Smith, 1977) to (Dow, 1991) and from (Yao, 2003) to Benson, 2011) have studied about local collapses such as tripping of stiffeners, stiffeners local buckling and ultimate strength of stiffened plates/panels and global hull collapses under in-plane and lateral loads theoretically, numerically and experimentally.

A series of tests and FEM analysis on full scale welded steel grillages subjected to a combination of axial compression and lateral pressure is presented by (Smith, 1976).

Efforts on experimental investigation for stiffened panel collapse behaviors were made by many researchers. The early works extended by (Paik et al., 2001, 2002, 2008) provide an extensive contribution to the ultimate strength evaluations for stiffened panels and hull girders by developing practical methods, codes and empirical formulas. (Benson, 2011) investigated aluminum stiffened panels' and ships' behaviors under uniaxial compressive loads and developed a semi-analytical method by using FEA and orthotropic plate theory.

2 METHODOLOGY

The progressive collapse method applied to ship hull girders by Smith Method (Smith, 1977), also basis of our solution methodology, is one of the simplified and most well recognized methods in the marine field to estimate the global strength of a hull girder. For a progressive collapse type analysis by Smith Method, the hull girder is usually discretized into plate-stiffener combination beam-column components. Failure of the hull girder in overall bending occurs by inter-frame failure of these components.

Another successful method to estimate the ultimate hull girder strength is idealized structural unit method (ISUM) developed by Ueda and Rashed (1991). For an ISUM type analysis the hull girder is usually discretized into several different types of structural members such as support members (single stiffeners), beam-columns, rectangular plates and stiffened panels.

The Smith method is developed into various registered computer codes by researchers. These codes use the same underlying methodology but differ in their approach to derive the load-end shortening curves.

The considered method presented in this study is composed from ISUM based component discretization and Smith Method based progressive collapse analysis. Unlike the application of conventional Smith method, single plate, single stiffener and stiffened panel components are also used instead of using just plate-stiffener combination beam-column components.

Developed systematic calculation method has two main advantages. First, large deflection orthotropic plate approach is extended by changing calculation technique. The traditional orthotropic plate method is closed form and it just give the result of ultimate strength. It doesn't directly calculate the historical load-shortening behavior of the panel under progressively increasing compressive load. Briefly, the extended calculation derives the complete panel load-shortening curve by different methods and uses the orthotropic panel approach to define the curve peak value. Second, depending on first advantage, using stiffened panel components instead of discretizing the complex hull entirely to stiffener-plate combination beam-column components, provide small number of discretized element. The small number components means small number load-shortening curves to be considered. This case reduces the analysis time. Thus, the disadvantage of using less component for progressive collapse analysis is also eliminated by considering the stress-strain behavior of stiffener and plate component individually during calculations.

However, discretizing relatively simple hulls to more components than other methods causes little increase to analysis time. Disadvantage of this is eliminated by using more single components and thus obtaining more realistic results.

Besides, another important point should be underlined that considering all collapse modes for stiffened panels by extended orthotropic plate large deflection approach provides the opportunity to make more realistic assessments.

In this study, according to HULT solution methodology all five modes for stiffened panel collapse are considered separately and accepted that collapse of stiffened panels occurs at the lowest value among the various ultimate loads.

In HULT, the load-end shortening curve relationships of structural components of hull girders under vertical bending moment are determined by numerically, empirically and semi-analytically. For these calculations "limit state design approach", "membrane stress approach", orthotropic panel approach" and the rules of IACS-CSR, 2012 are used. The stress-strain behaviors of initially deflected single plates, single stiffeners, plate-stiffener combination components with different type and geometry and stiffened panel components are obtained by von-Karman & Marguerre plate equations, IACS-CSR single step procedure with simplified analytical formulas and updated orthotropic panel approach calculations, respectively. Then, the progressive collapse calculations are performed using the determined load-end shortening curves.

Within the method, the historical single stiffener strength values are determined by comparison of standard stress-strain curves derived from IACS-CSR equations and non-linear FEM analysis. The historical unstiffened plate strength values are determined by comparison of standard stress-strain curves derived by using Marguerre governing large deflection nonlinear equations of initially deflected single plate theory extended from von Karman's original equilibrium and compatibility equations and non-linear FEM analysis. The plate-stiffener combination beam-column components' strength values are determined by combining the plate and stiffener strength obtained from above mentioned curves and a comparison is conducted with plate-stiffener combination buckling strength evaluation using standard stress-strain curves derived from IACS-CSR equations and non-linear FEM analysis.

The stiffened panel components' load-end shortening (stress-strain) behaviors behind and beyond ultimate strength are obtained by updated orthotropic panel calculation procedure but using historical combined stress-strain curves of several type single stiffeners and single plates mentioned in paragraph above. The overall panel strength between two adjacent frames (not for whole ship) is evaluated by large deflection orthotropic panel approach but using renewed instantaneous longitudinal geometric properties like Ex, Dx determined by instantaneous tangent modulus ET,p and Et,s from the plate components' and stiffener components' load shortening curves, respectively. Details of this procedure and obtaining the load-end shortening curves of other single components can be find from study of (Benson, 2011) and (Ölmez, 2014). The sample of calculation flowchart for orthotropic panel historical P-du derivation can be seen from Fig. 2.

Historical relation between the bending moment acting on the cross section and curvature formed in this section is determined as a result of method. The peak value of this curve is accepted as ultimate strength of ship. According to the theory of the method, in the absence stress or strain on the hull section neutral axis, its length remains constant. Since the curvature depending on moment along the length of the calculation part remains constant, the neutral axis takes the $1/\kappa$ radius circle arc form. Besides, there are rotations occurs as the angle θ at both side of hull section, because of the main acceptation that plane sections remain plane and perpendicular to neutral axis.

The distance between neutral axis and intersection point of original and rotated cross sections gives curvature radius. The definition sketch for the forced curvature principle under the case of pure bending is shown in Fig 3.

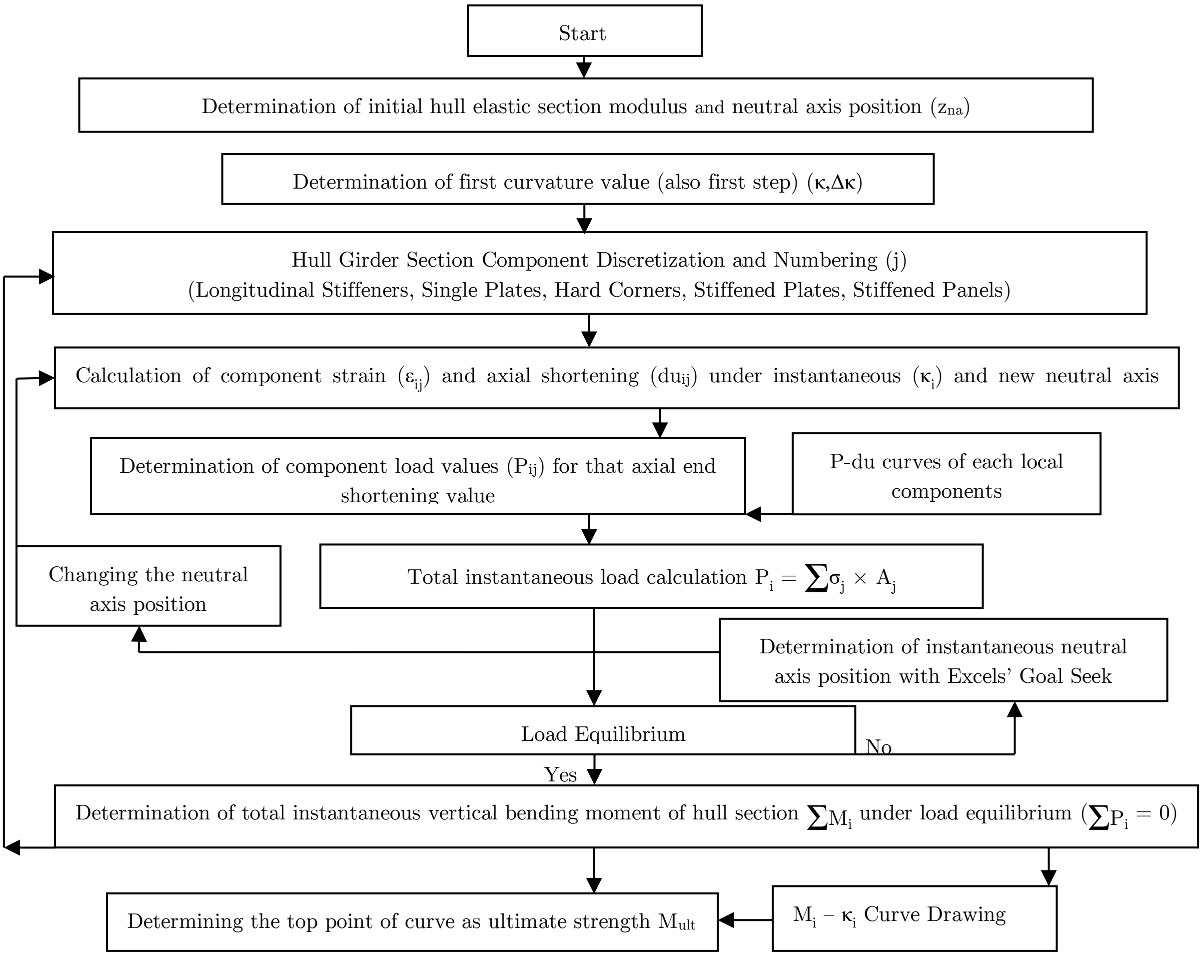

Figure 2: Calculation flowchart for orthotropic panel historical P-du derivation.

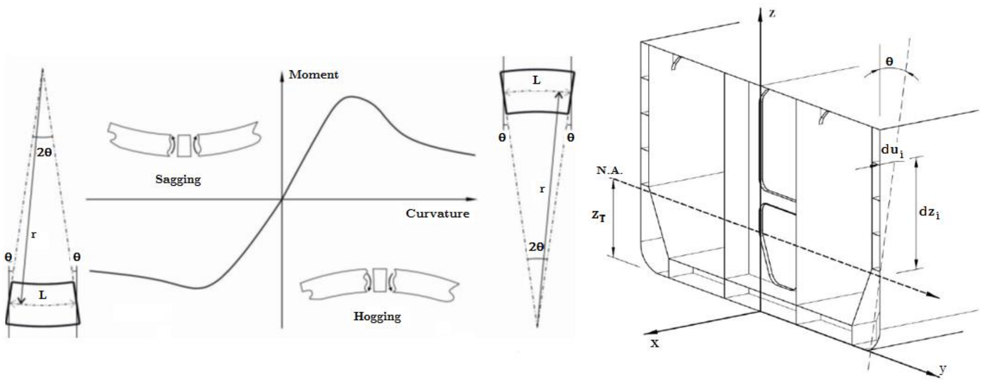

Figure 3: Definition sketch for the forced curvature principle in the case of pure bending (Özgüç, 2006).

The load-end shortening curves obtained previously will be used instead of average stress- average strain curves for the progressive hull collapse calculations to plot moment-curvature curve. Physically, these curves shows that how much internal forces will be created by axial straining of that structural component. After large deflection analysis of components, the progressive collapse calculation starts with approximately calculated curvature depending on vertical bending moment given by a linear elastic bending stress of yield, modulus of elasticity and specified minimum yield stress of the material. Next, the strain distribution ($\varepsilon_{ij} = \kappa_i \times \Delta z_{ij}$) can be calculated depending on the curvature (κ_i) and distance from neutral axis (Δz_{ij}). Afterwards, the axial end shortening (du_{ij}) can be calculated with the aid of strain distribution on the section. The instantaneous load corresponds to the axial displacement value of the component is read from load-shortening (P-du) curve and written in the calculation Table 1 prepared for progressive hull collapse analysis.

	Instantaneous Curvature		κ_i	Instantaneous Neutral Axis Position		z_{Ti}
Comp. No	z_{ij}	Δz_{ij}	ε_{ij}	du_{ij}	P_{ij}	M_{ij}
j : 1,2,3	z_{ij}	$z_{ij} - z_{Ti}$	$\varepsilon_{ij} = \kappa_i \times \Delta z_{ij}$	$\varepsilon_{ij} \times L$	From P-du curves	$P_i \times \Delta z_{ij}$
	i : iteration number ; j : component number				$\Sigma P_i = 0$	ΣM_i

Table 1: Progressive hull collapse analysis calculation table.

During the calculation process with Table 1, in each calculation step (each curvature increment) the total internal loads (ΣP_i) of each components (P_{ij}) of the hull section have to be zero for equilibrium. If the balance has not been achieved, it indicates that the position of the neutral axis should be changed to calculate the strain values correctly under instantaneous curvature. To determine the position of neutral axis providing equilibrium, the sub-calculation is made with Excel Goal Seek. Next, the moments (M_{ij}) are calculated by multiplying the load (P_{ij}) and vertical distance of component from neutral axis (Δz_{ij}) and the total hull section bending moment (ΣM_i) is obtained by sum of each components moment values.

3 SHIPS OF VERIFICATION BENCHMARK STUDIES ON ULTIMATE HULL GIRDER STRENGTH

The accuracy of ultimate strength estimations of ship hull girders is now examined with the objective of validating HULT's ultimate strength procedures for ship and offshore structures. This is accomplished through evaluations of ten benchmark case studies for which detailed structural information and associated numerical or measured results are reported in literature. The main geometric properties and mid-ship sections of considered ten benchmark ships are represented in next subsections.

3.1 Cross Sections and Structural Characteristics

In this part, the characteristics of progressive collapse behavior of ten benchmark ships under vertical sagging or hogging are investigated using the HULT code and shown in Table 2.

No	Ship Type	Abbreviation	Reference
1	1/3 Scale Frigate	FRG	Dow, 1991
2	Single Hull VLCC Oil Tanker (Energy Concentration)	SHOT	Rutherford and Calwell,1990
3	3,500 TEU Container	CNT35	ISSC, 2000
4	47,326 DWT Double Hull Oil Tanker	DHOT1	Dalma, 2009
5	105,000 DWT Double Hull Oil Tanker	DHOT2	Paik et al., 2002
6	313,000 DWT Double Hull Oil Tanker	DHOT3	Paik et al., 2002
7	170,000 DWT Single Sided Bulk Carrier	SSBC	Paik et al., 2002
8	169,000 DWT Double Sided Bulk Carrier	DSBC	Paik et al., 2002
9	9,000 TEU Container	CNT90	Paik et al., 2002
10	113,000 DWT Floating Production Storage and Offload	FPSO	Paik et al., 2002

Table 2: Considered ten benchmark typical ships.

The cross sections of ten ships and main hull section properties are shown in Fig. 4 and Table 3, respectively.

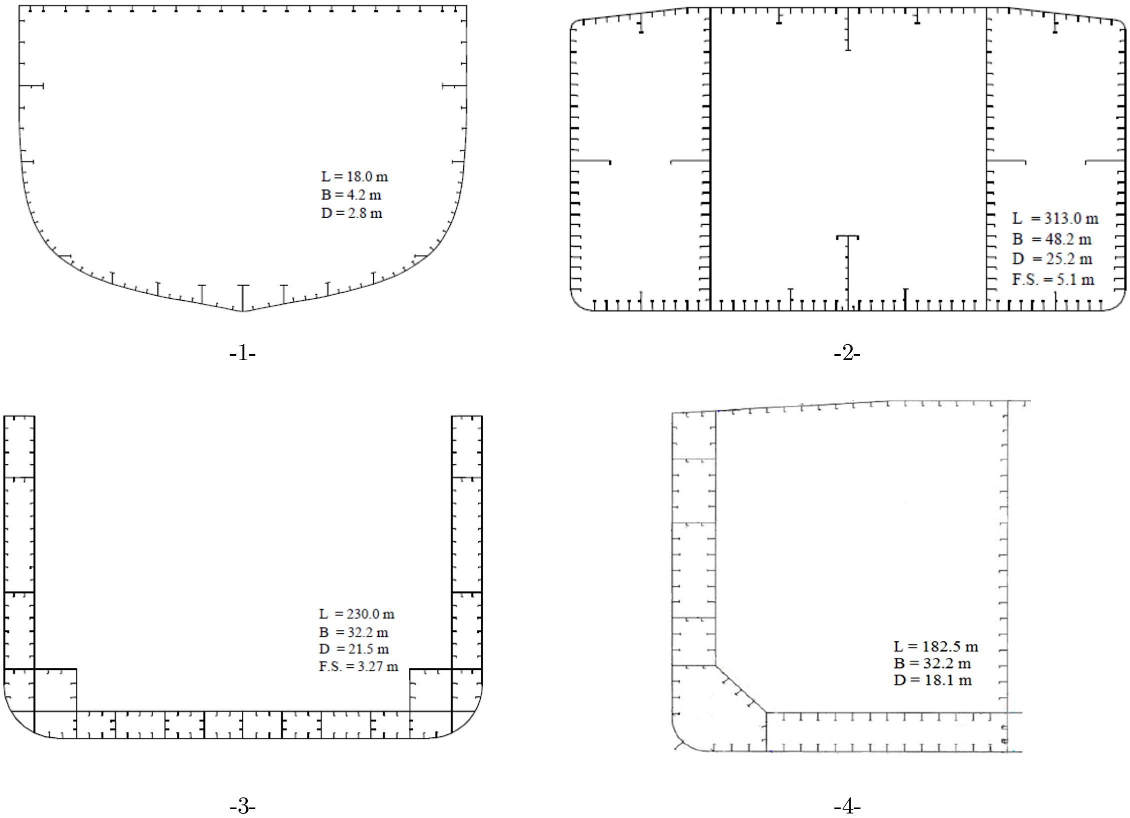

Figure 4: Mid-ship cross sections of ten benchmark ships (1 - 4).

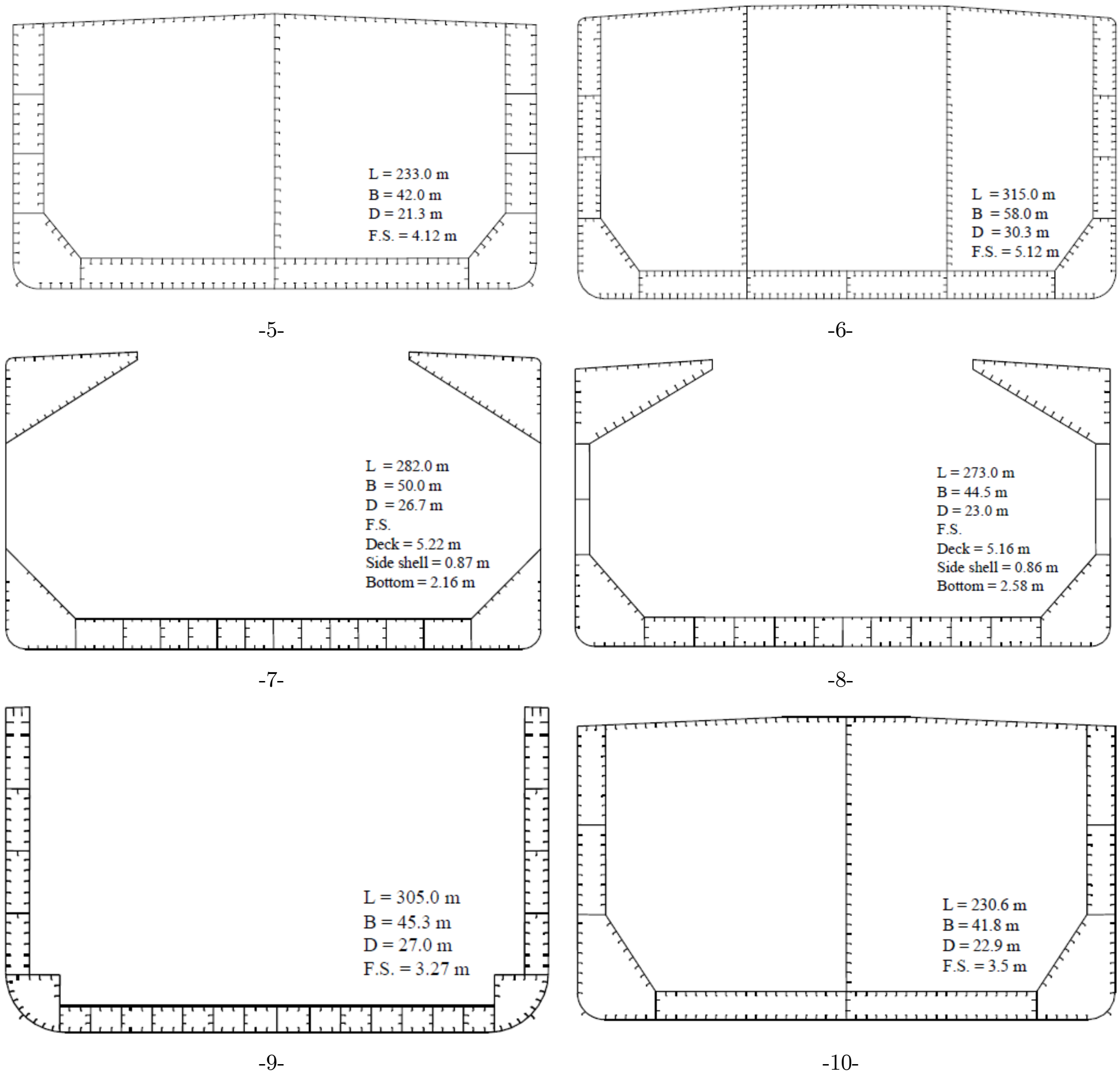

Figure 4 Cont.: Mid-ship cross sections of ten benchmark ships (5 - 10).

Hull Sec. Prop.		FRG	SHOT	CNT35	DHOT1	DHOT2	DHOT3	SSBC	DSBC	CNT90	FPSO
Length (m)		18	313	230	182.5	233	315	282	273	305	230.6
Breadth (m)		4.2	48.2	32.2	32.2	42	58	50	44.5	45.3	41.8
Depth (m)		2.8	25.2	21.5	18.1	21.3	30.3	26.7	23	27	22.9
Draft (m)		-	19	12.5	12.6	12.2	22	19.3	15	13.5	14.15
C_b		-	0.83	0.68	0.77	0.83	0.82	0.83	0.84	0.65	0.83
Cross Sec. Area (m^2)		-	7.85	3.84	3.02	5.31	9.63	5.65	5.78	6.19	4.88
Neutral Axis (m)		1.42	12.1	8.50	7.68	9.18	12.97	11.18	10.05	11.61	10.21
I (Vertical) (m^4)		0.06	863.7	237.5	164.8	359.5	1346.1	694.3	508.3	682.8	393.6
Z (m^3)	Deck	0.03	66.30	18.33	13.81	29.68	77.24	44.35	39.27	44.37	31.04
	Bottom	0.04	70.95	27.23	18.72	39.13	103.77	62.06	50.54	58.78	38.52
σ_y MPa	Deck	245	315	355	245	315	315	390	355	355	315
	Bottom	245	315	315	315	315	315	315	315	315	315

Table 3: Principal dimensions of the ten benchmark typical ship hull sections.

3.2 Progressive Hull Collapse Analysis and Calculated Results

The ultimate vertical bending moment of the ten hull structures are estimated using HULT and IACS-CSR/KTU (Ölmez, 2014). The results are compared with published results (Dow, 1991), (ISSC, 2000), (Paik et al., 2002), (Özgüç, 2006), (Dalma, 2009), (Tayyar, 2011), (Benson, 2011), (ISSC 2012), (Andric et al., 2014). It is noted that the hull structural dimensions applied for all analysis were defined by including 50% corrosion margin (0.5 x t_{corr}) values of individual structural components as specified by IACS-CSR (2012), which ensures obtained results as incomparable with all other results. Fig. 5 shows three of discretized IACS-CSR and HULT models employed for the progressive hull collapse analysis under vertical bending within this study. A small but enough to represent part of hull cross-section model between two adjacent transverse frames at mid-ship is adopted as the extent of the analysis. For HULT code modelling, structural components between support members are idealized such as single stiffeners (longitudinal support members excluding attached plating), single plates, single stiffeners with attached plating (beam-column components), hard corners and identically stiffened panels. Firstly, 45 beam-column (PSC), 2 hard corner (K) and 3 single plate (P) components are used in FRG/IACS-CSR and 1 stiffened plate (SP), 2 beam-column, 37 single stiffener (S), 33 single plate and 5 hard corner components are used in FRG-HULT. Second, 110 beam-column, 6 single plate and 16 hard corner components are used in SHOT/IACS-CSR and 25 stiffened plate, 30 single plate, 22 single stiffener and 33 hard corner component are used in SHOT/HULT. At last, 82 beam-column and 62 hard corner components are used in CNT35/IACS-CSR and 32 stiffened plate, 8 single plate, 10 single stiffener and 60 hard corner components are used in CNT35/HULT.

The main assumptions used for ten hull girder progressive collapse calculations are:

1- Analysis are carried out between two adjacent transverse frames.

2- Plane sections remains plane after bending (Euler-Bernoulli Bending Theory).

3- The neutral axis of the hull cross section changed as the collapse of individual structural components progressively occurs. For example, if the discretized structural components from deck are collapse first, the neutral axis position moves downwards to provide equilibrium and stability at current load step. The opposite is also true. Decrease or increase of the neutral axis position according to hogging or sagging case is taken into account as the vertical bending moment is increasingly applied.

4- Average level ($0.15 \times \sigma_{yield}$) welding residual stress is considered (Smith et al., 1988) in benchmark study of ten ships and benchmark study of component discretization effects for validation. Next, two more welding residual stress levels (slight and severe) are considered in benchmark study of initial distortion effects to investigate their effects on structural components' behaviors and ultimate strength results.

5- Buckling mode average level initial out of plane deflection ($0.1 \times \beta^2 \times t$) is considered (Smith et al., 1988) in benchmark study of ten ships and benchmark study of component discretization effects for validation. Next, two more initial deflection levels (slight and severe) are considered in benchmark study of initial distortion effects to investigate initial out of plane deflection effects on structural components' behaviors and ultimate strength results.

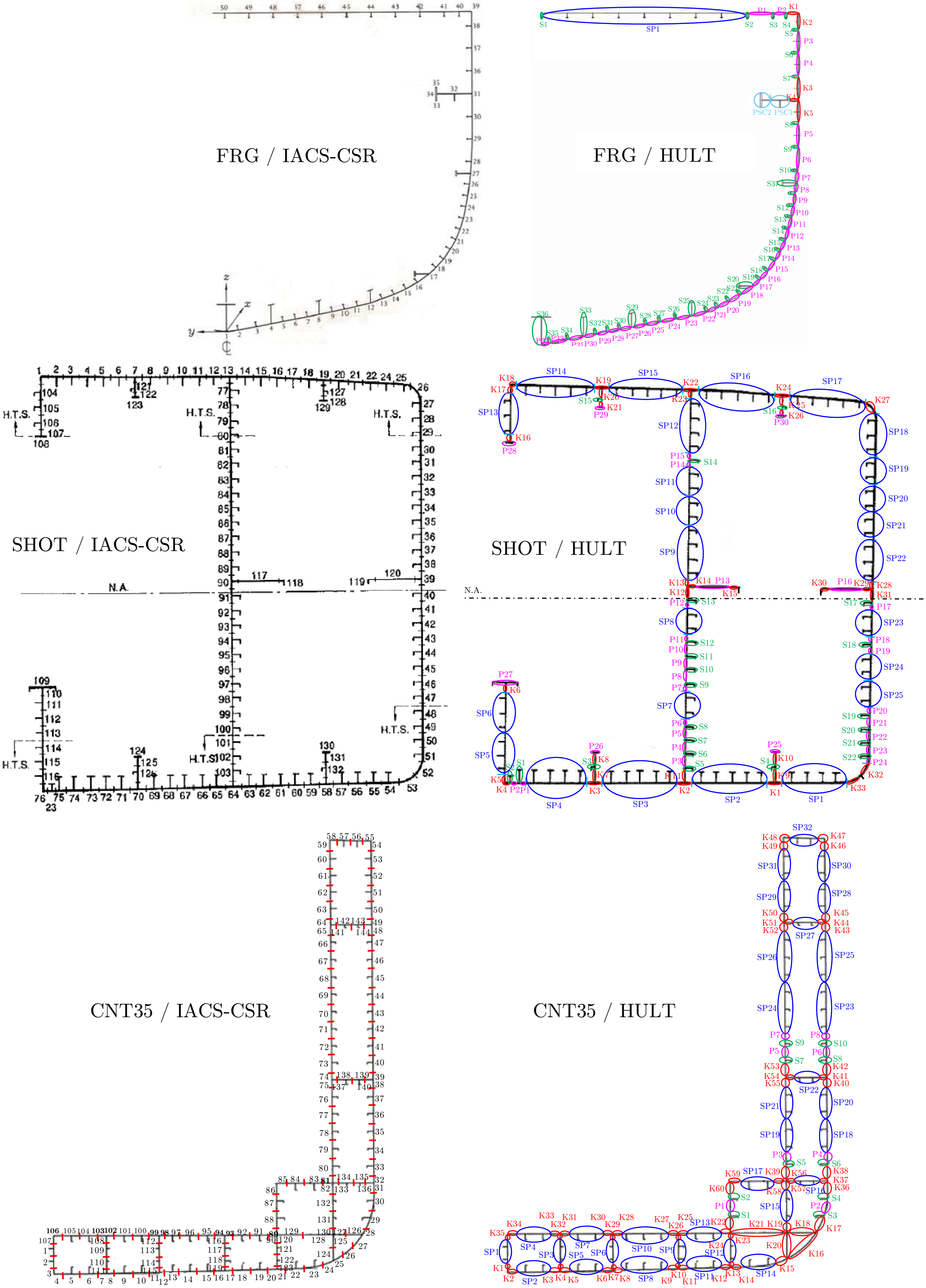

Figure 5: Component discretization of FRG, SHOT and CNT35 with HULT and IACS-CSR.

The result comparison of hogging and sagging condition ultimate strength calculations with HULT, IACS-CSR and published other results obtained by different authors using various methods are comparatively represented in Table 4 and Fig. 6, respectively. Next, effects of hull girder section component discretization, initial deflection of plates and residual welding stress as initial distortions, and 50% corrosion margin for individual structural components on ultimate hull girder strength are represented by table and graphs in benchmark studies below.

$M_{ultimate}$ ($x10^3$ kNm for model FRG & $x10^6$ kNm for models SHOT to DHOT2)	Remarks	FRG		SHOT		CNT35		DHOT1		DHOT2	
		Hog.	Sag.	Hog.	Sag.	Hog.	Sag.	Hog.	Sag.	Hog.	Sag.
1.	Chen [ISSC,2000]	12.49	9.54	20.23	18.54	6.56	5.47	-	-	-	-
2.	Cho [ISSC,2000]	11.32	9.48	20.09	16.75	6.69	5.13	-	-	-	-
3.	Masaoka [ISSC,2000)]	12.49	11.50	20.01	19.00	8.07	7.95	-	-	-	-
4.	Rigo(1) [ISSC,2000]	13.26	9.47	18.46	17.90	7.60	6.51	-	-	-	-
5.	Rigo(2) [ISSC,2000]	12.12	9.88	17.54	17.10	7.20	6.91	-	-	-	-
6.	Yao [ISSC,2000]	10.90	8.58	19.03	16.84	6.72	6.72	-	-	-	-
7.	ALPS/HULL [Paik,2002]	10.45	9.94	16.77	15.83	6.92	6.64	-	-	8.49	6.90
8.	Paik-FEM [ISSC,2012]	-	9.62	17.36	16.18	6.97	6.95	-	-	-	-
9.	Mod. P-M [ISSC,2012]	-	-	18.70	17.83	6.4	7.08	-	-	-	-
10.	Benson [2011]	-	10.20	-	-	-	-	-	-	-	-
11.	Dalma [2009]	-	-	-	-	-	-	-	3.09	-	-
12.	ISR-FEM [ISSC,2012]	-	-	21.2	20.2	7.49	7.18	-	-	-	-
13.	CR-FEM [ISSC,2012]	-	-	21.86	20.63	7.66	7.63	-	-	-	-
14.	Özgüç [2006]	12.01	9.60	17.89	16.45	6.79	6.70	-	-	-	-
15.	Tayyar [2011]	-	9.74	17.02	-	-	-	-	-	-	-
16.	Dow [1991]	11.39	9.64	18.80	-	-	-	-	-	-	-
17.	Ruth-Caldwell [ISSC,2000]	-	-	17.94	-	-	-	-	-	-	-
18.	CSR-CR [ISSC,2012]	-	-	20.71	18.59	7.88	7.59	-	-		
19.	CSR-PNU [ISSC,2012]	-	-	20.10	18.71	7.76	6.85	-	-		
20.	Rina Rules [ISSC,2012]	-	-	19.84	18.47	6.86	5.90	-	-		
21.	CSR-FSB [Andric et al., ,2014]	-	-	19.41	18.30	7.58	6.82	-	-		
22.	CSR-KTU [Ölmez,2014]	12.11	10.25	19.30	18.03	7.25	6.65	4.88	2.97	8.75	6.95
23.	HULT	12.18	9.53	17.66	16.95	7.34	6.68	5.26	3.25	8.61	7.08
Mean / All Methods		11.86	9.784	19.04	17.91	7.21	6.74	5.07	3.10	8.62	6.98
St.Dv. / All Methods		0.841	0.633	1.416	1.314	0.492	0.702	0.269	0.140	0.13	0.09
COV / All Methods		0.071	0.065	0.074	0.073	0.068	0.104	0.053	0.045	0.013	0.018
COV / Smith Based		0.060	0.087	0.062	0.049	0.069	0.115	0.053	0.064	0.014	0.013

Table 4: Summary of benchmark ship's ultimate bending moment results for all methods.

	Remarks	DHOT3		SSBC		DSBC		CNT90		FPSO	
		Hog.	Sag.	Hog.	Sag.	Hog.	Sag.	Hog.	Sag.	Hog.	Sag.
$M_{ultimate}$ (x10^6 kNm for models DHOT3 to FPSO)	1. Chen [ISSC,2000]	27.40	24.33	19.06	15.20	-	-	-	-	-	-
	2. Cho [ISSC,2000]	28.66	20.80	18.99	13.69	-	-	-	-	-	-
	3. Masaoka [ISSC,2000)]	30.59	26.59	18.56	16.02	-	-	-	-	-	-
	4. Rigo(1) [ISSC,2000]	28.32	19.57	18.71	14.34	-	-	-	-	-	-
	5. Rigo(2) [ISSC,2000]	25.61	24.07	17.06	14.34	-	-	-	-	-	-
	6. Yao [ISSC,2000]	28.88	20.42	17.36	14.45	-	-	-	-	-	-
	7. ALPS/HULL [Paik et al., 2002]	23.59	19.57	16.60	15.38	12.03	12.2	13.08	16.60	8.76	7.28
	8. Paik-FEM [ISSC,2012]	27.34	22.50	17.50	15.80	-	-	-	-	-	-
	9. Mod. P-M [ISSC,2012]	25.67	22.39	16.58	14.8	-	-	-	-	-	-
	10. Benson [2011]	-	-	-	-	-	-	-	-	-	-
	11. Dalma [2009]	-	-	-	-	-	-	-	-	-	-
	12. ISR-FEM [ISSC,2012]	30.11	28.18	18.33	17.73	-	-	-	-	-	-
	13. CR-FEM [ISSC,2012]	31.00	25.00	18.40	16.86	-	-	-	-	-	-
	14. Özgüç [2006]	27.45	21.15	17.34	14.19	-	-	-	-	-	-
	15. Tayyar [2011]	-	-	-	-	-	-	-	-	-	-
	16. Dow [1991]	-	-	-	-	-	-	-	-	-	-
	17. Ruth.-Caldwell [ISSC, 2000]	-	-	-	-	-	-	-	-	-	-
	18. CSR-CR [ISSC,2012]	29.85	25.01	18.34	14.92	-	-	-	-	-	-
	19. CSR-PNU [ISSC,2012]	28.42	22.13	18.36	14.50	-	-	-	-	-	-
	20. Rina Rules [ISSC,2012]	28.20	21.67	17.48	13.95	-	-	-	-	-	-
	21. CSR-FSB [Andric et al., 2014]	28.43	21.16	17.87	14.19	-	-	-	-	-	-
	22. CSR-KTU [Ölmez,2014]	28.11	20.58	18.05	14.65	12.28	12.88	14.35	16.18	9.55	7.74
	23. HULT	24.59	21.55	17.45	15.12	11.76	12.69	13.88	16.74	9.30	7.46
Mean / All Methods		28.01	22.62	17.89	15.01	12.02	12.25	13.77	16.51	9.202	7.491
St.Dv. / All Methods		1.798	2.426	0.758	1.044	0.260	0.410	0.642	0.291	0.402	0.234
COV / All Methods		0.064	0.107	0.042	0.069	0.022	0.034	0.047	0.018	0.041	0.032
COV / Smith Based		0.056	0.101	0.037	0.042	0.031	0.047	0.024	0.020	0.018	0.019

Table 4 Cont.: Summary of benchmark ship's ultimate bending moment results for all methods.

Results obtained by methods 1 to 6, 10, 14, 15 and 18 to 23 were considered for calculation of Mean, St. Dv. and COV values of Smith Based (different formulations for obtaining the load-end shortening curves) calculations. Coefficient of variation (COV) calculated for all methods and Smith based methods are given in Table 3. COV for all methods varies from 0.013 to 0.107 and COV for Smith based methods varies from 0.013 to 0.115. Average COV calculated for considered groups are

0.053 and 0.049, respectively. This decreasing on average COV shows that similarity of methods increases as expected. It can also be noted that closed results are obtained by various Smith based methods (1 to 6, 10, 14, 15, 20 and 23) and the IACS-CSR method implementations use same formulations for load-end shortening curves (18, 19, 21 and 22).

Although standard formulations for standard component idealization, there are small differences among CSR results due to researcher factors (code algorithm, structural discretization, assumptions, etc.).

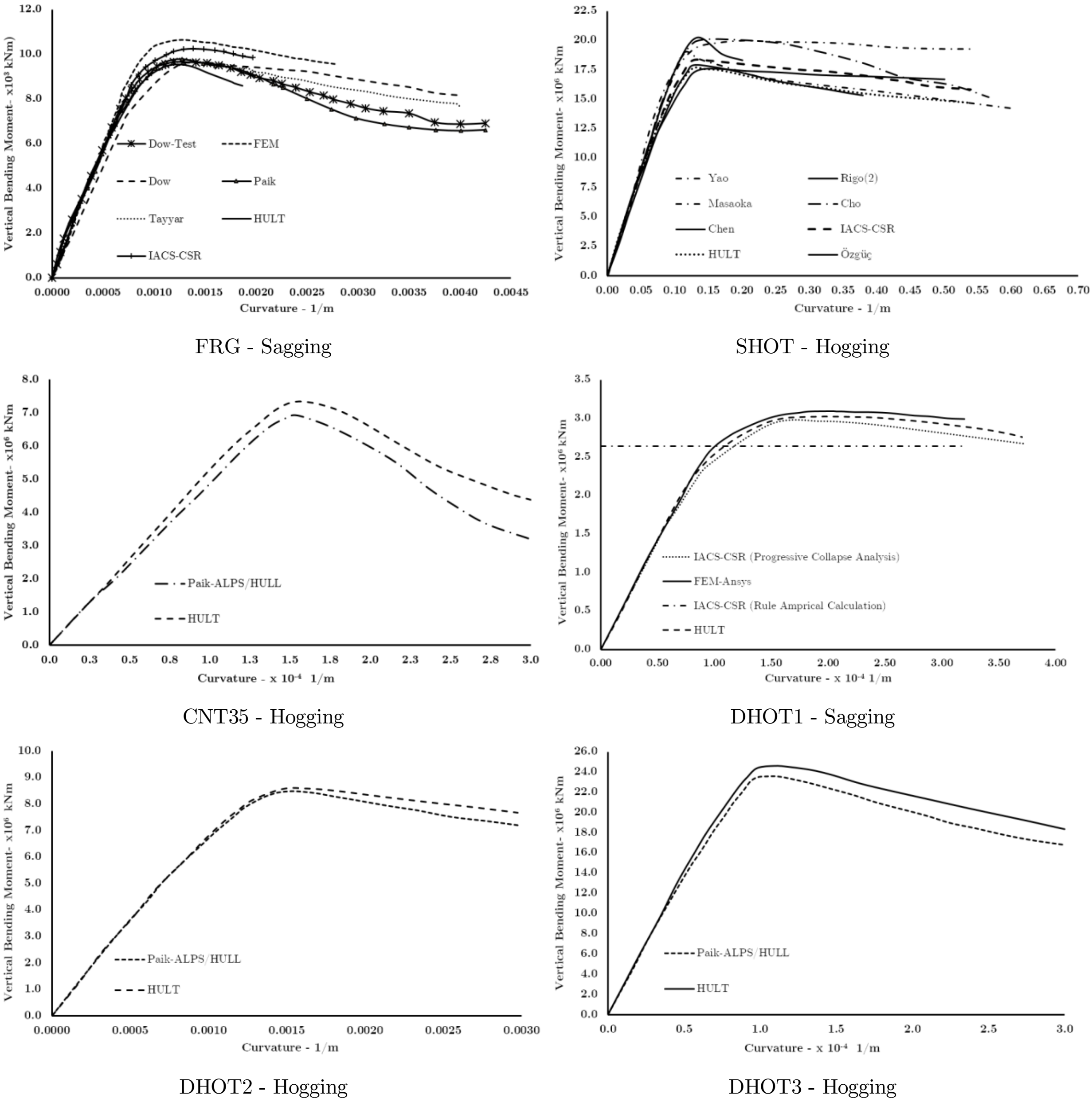

Figure 6: Moment-curvature curves of model 1 to 6.

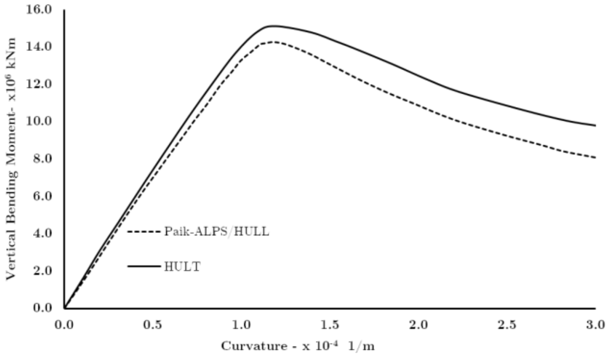

SSBC - Sagging

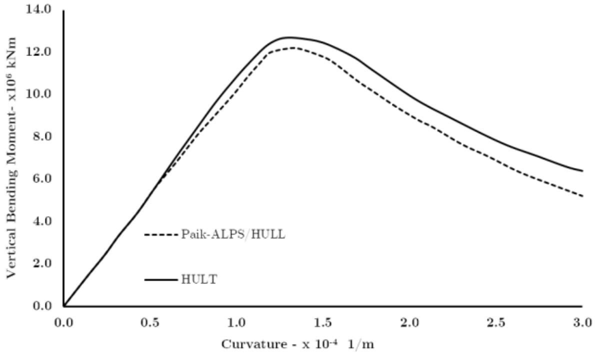

DSBC - Sagging

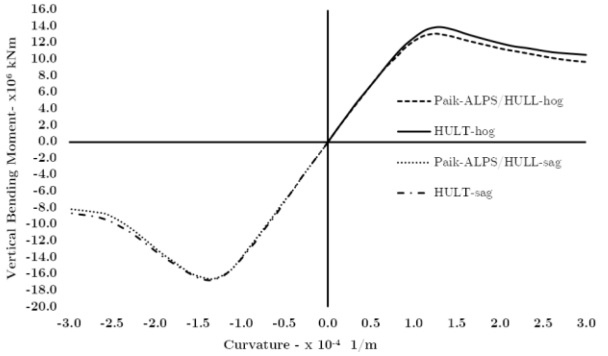

CNT90 - Sagging / Hogging

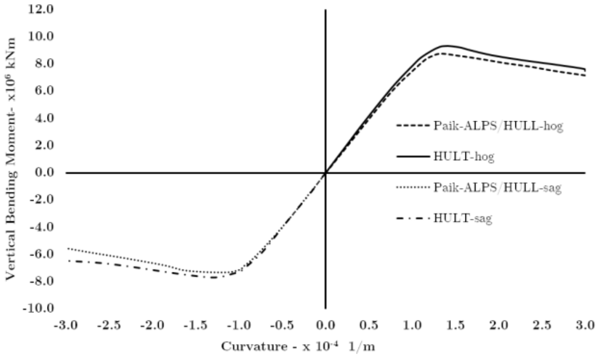

FPSO - Sagging / Hogging

Figure 6 Cont.: Moment-curvature curves of model 7 to 10.

3.3 Benchmark Study for Component Discretization Effect

The ultimate vertical bending moment of the five hull structures are estimated using HULT with three different component discretization, then the results are compared with each other and published results. It is noted that the hull structural dimensions applied for the all analysis were defined by including 50% corrosion margin ($0.5 \times t_{corr}$) values of individual structural components as specified by IACS-2012, which ensures obtained results as incomparable with all other results.

Also, average level welding residual stresses ($0.15x\sigma_0$) and buckling mode average level initial deflection ($0.1 \times \beta^2 \times t$) is considered. Based on the structural idealization techniques (Hughes and Paik, 2010), three types of HULT modelling are considered for all benchmark ships. As the extent of the analysis, all three models take a single hull segment between two adjacent transverse frames. Model I idealizes the structure by only the plate-stiffener combination components (beam-column units). In Model II, the entire hull structure is idealized by the plate-stiffener separation components. While deck, bottom, side and longitudinal bulkhead parts that have identical stiffener and plate components in Model III are modelled as the stiffened panel components. Other components for Model III are idealized as plate-stiffener separation components.

The result comparison of hogging and sagging condition ultimate strength calculations with HULT, IACS-CSR and published other results obtained by different authors using various methods are comparatively represented in Table 5 and Fig. 7, respectively.

$M_{ultimate}$ ($x10^3$ kNm for model FRG & $x10^6$ kNm for models SHOT to SSBC)

Remarks	FRG		SHOT		CNT35		DHOT2		SSBC	
	Hog	Sag	Hog	Sag	Hog	Sag	Hog	Sag	Hog	Sag
1. Chen [ISSC,2000]	12.49	9.54	20.23	18.54	6.56	5.47	-	-	19.06	15.20
2. Cho [ISSC,2000]	11.32	9.48	20.09	16.75	6.69	5.13	-	-	18.99	13.69
3. Masaoka [ISSC,2000]	12.49	11.5	20.01	19.00	8.07	7.95	-	-	18.56	16.02
4. Rigo (2) [ISSC,2000]	12.12	9.88	17.54	17.10	7.20	6.91	-	-	17.06	14.34
5. Yao [ISSC,2000]	10.90	8.58	19.03	16.84	6.72	6.72	-	-	17.36	14.45
6. ALPS/HULL [Paik et al.,2002]	10.45	9.94	16.77	15.83	6.92	6.64	8.49	6.90	16.60	14.28
7. Paik-FEM [ISSC,2012]	-	9.62	17.36	16.18	6.97	6.95	-	-	17.50	15.80
8. Modified P-M [ISSC,2012]	-	-	18.70	17.83	6.4	7.08	-	-	16.58	14.8
9. ISR-FEM [ISSC,2012]	-	-	21.2	20.2	7.49	7.18	-	-	17.06	14.34
10. CR-FEM [ISSC,2012]	-	-	21.86	20.63	7.66	7.63	-	-	17.36	14.45
11. Ozguc [2006]	12.01	9.60	17.89	16.45	6.79	6.70	-	-	16.60	15.38
12. Tayyar [2011]	-	9.74	17.02	-	-	-	-	-	17.50	15.80
13. Dow [1991]	11.39	9.64	18.80	-	-	-	-	-	16.58	14.8
14. Ruth.-Caldwell [ISSC, 2000]	-	-	17.94	-	-	-	-	-	17.06	14.34
15. CSR-CR [ISSC,2012]	-	-	20.71	18.59	7.88	7.59	-	-	17.36	14.45
16. CSR-PNU [ISSC,2012]	-	-	20.10	18.71	7.76	6.85	-	-	16.60	15.38
17. Rina Rules [ISSC, 2012]	-	-	19.84	18.47	6.86	5.90	-	-	17.50	15.80
18. CSR-FSB [Andric et al.,2014]	-	-	19.41	18.30	7.58	6.82	-	-	16.58	14.8
19. CSR-KTU [Olmez, 2014]	12.11	10.2	19.30	18.03	7.25	6.65	8.75	6.95	17.06	14.34
HULT- Model I	12.35	9.61	18.09	17.15	7.47	6.85	8.79	7.21	17.88	15.68
HULT-Model II	12.05	9.46	17.38	16.80	7.29	6.55	8.25	6.84	16.75	14.73
HULT-Model III	12.18	9.53	17.66	16.95	7.34	6.68	8.61	7.08	17.45	15.12
Mean	11.82	9.737	18.95	17.81	7.205	6.750	8.578	6.99	17.32	14.91
St.Dv.	0.656	0.621	1.435	1.311	0.473	0.682	0.218	0.14	0.743	0.642
COV	0.055	0.064	0.076	0.074	0.066	0.101	0.025	0.02	0.043	0.043

Table 5: Summary of benchmark ship's ultimate bending moment results for all methods.

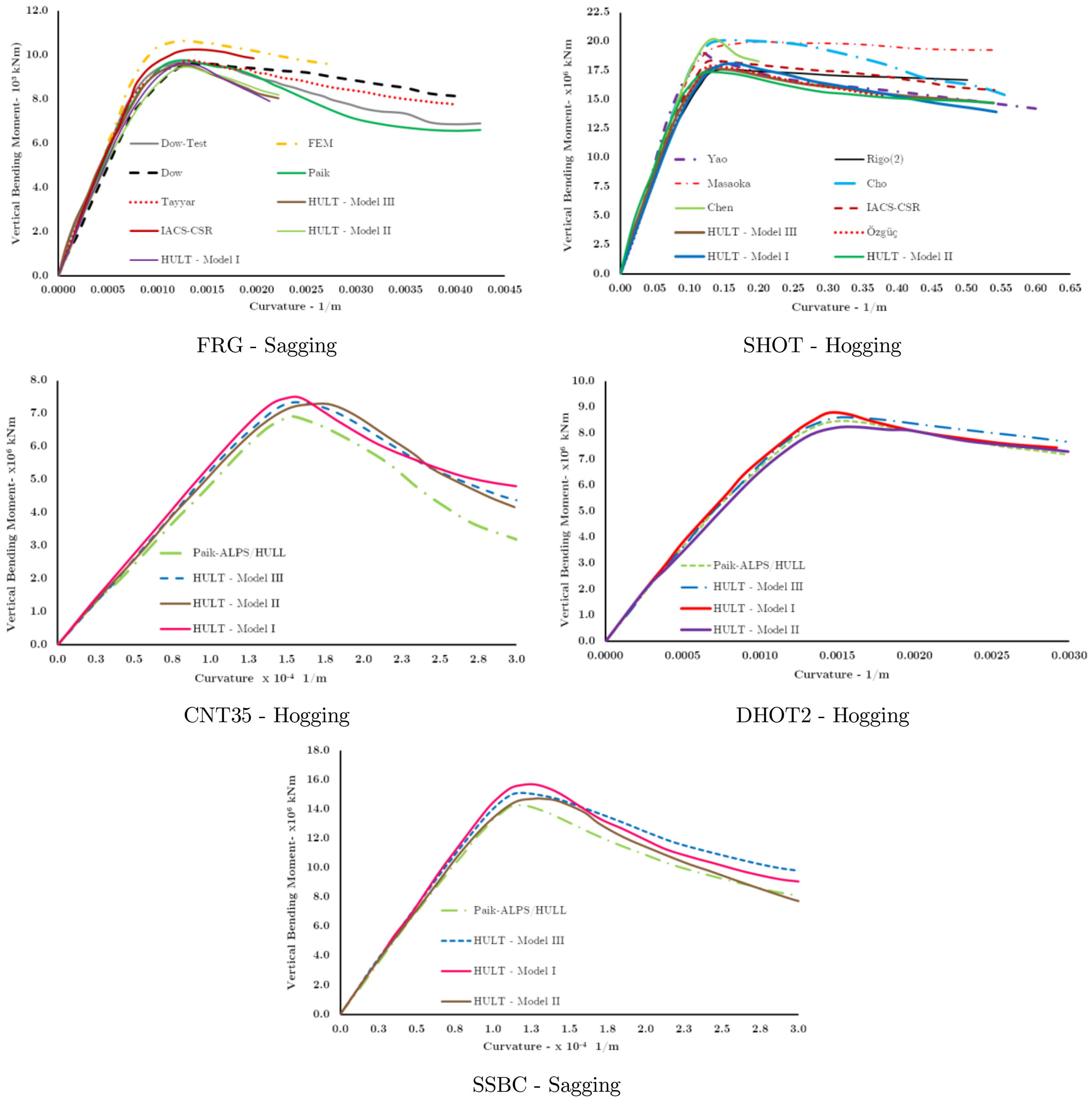

Figure 7: Moment-curvature curves of five benchmark ships.

3.4 Benchmark Study for Initial Distortion Effects

In this benchmark study, to test the reliability of the HULT one more time and also to investigate the effects of initial distortions including initial deflections, residual welding stresses and plate thickness decrease due to corrosion on ultimate hull girder strength, a typical 3,500 TEU double sided - double bottom container ship have ultimate strength results in literature is considered to calculate the ultimate hull girder strength with five different scenarios. The three level initial deflections and residual stresses values determined by Smith et al., 1988 are considered in calculations. These scenarios can be seen in Table 6.

Scenario No	w_0	σ_{rcx}	$t_{component}$
1	$0.025 \times \beta^2 \times t_p$	$-0.15 \times \sigma_{Yp}$	$t_{cor\text{-}ABS}$
2	$0.1 \times \beta^2 \times t_p$	$-0.15 \times \sigma_{Yp}$	$t_{cor\text{-}ABS}$
3	$0.3 \times \beta^2 \times t_p$	$-0.15 \times \sigma_{Yp}$	$t_{cor\text{-}ABS}$
4	$0.1 \times \beta^2 \times t_p$	$-0.05 \times \sigma_{Yp}$	$t_{cor\text{-}ABS}$
2	$0.1 \times \beta^2 \times t_p$	$-0.15 \times \sigma_{Yp}$	$t_{cor\text{-}ABS}$
5	$0.1 \times \beta^2 \times t_p$	$-0.3 \times \sigma_{Yp}$	$t_{cor\text{-}ABS}$

Table 6: Progressive collapse analysis scenarios.

A mid-ship section and perspective view of a typical double sided - double bottom container ship can be seen in Figure 8. The real mid-ship section of container ship with numbered structural components that the progressive collapse strength of the ship is calculated can be seen in Figure 9. Also, the geometrical and material specifications of longitudinal stiffener components of the mid-ship cross section are given in Table 7.

Figure 8: Typical 3,500 TEU double sided - double bottom container ship.

Stf. No	Web mm	Flange mm	Stif. Type	Mat. Yield MPa	Stf. No	Web mm	Flange mm	Stif. Type	Mat. Yield MPa
1	300 x 38		Flat	352.8	9	230 x 10		Flat	313.6
2	300 x 28		Flat	313.6	10	300 x 13	90 x 17	L	313.6
3	250 x 10	90 x 15	L	313.6	11	150 x 12	90 x 12	L	313.6
4	250 x 12	90 x 16	L	313.6	12	250 x 12	90 x 15	L	313.6
5	300 x 11	90 x 16	L	313.6	13	150 x 12		Flat	313.6
6	300 x 13	90 x 17	L	313.6	14	150 x 9	90 x 9	L	313.6
7	350 x 12	100 x 17	L	313.6	15	150 x 10		Flat	313.6
8	400 x 11.5	100 x 16	L	313.6	16	300 x 11	90 x 16	L	313.6

Table 7: Geometrical and material specifications of longitudinal stiffener components.

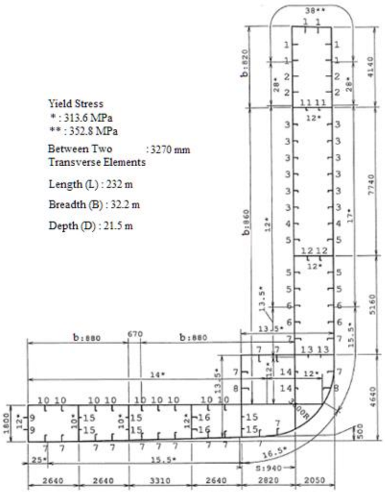

Figure 9: Mid-ship section of considered container ship.

High strength steel (σ_Y = 352.8 MPa) was used in deck, side and top two components portion of the double side. Relatively low-strength steel (σ_Y = 313.6 MPa) in the longitudinal members of the double side, bottom and double bottom was preferred. The length between two transverse support components that analysis conducted is 3.27 m. The distance between two stiffeners in upper part of the double-sides is preferred as 820 mm, in other parts of the double-side 860 mm and in double bottom 880 mm. Thickness of all structural components are determined by considering the corrosion effects and net thickness approach represented in IACS-CSR. The considered mid-ship section with 144 components by IACS-CSR and with 110 components by HULT are represented in Figure 10.

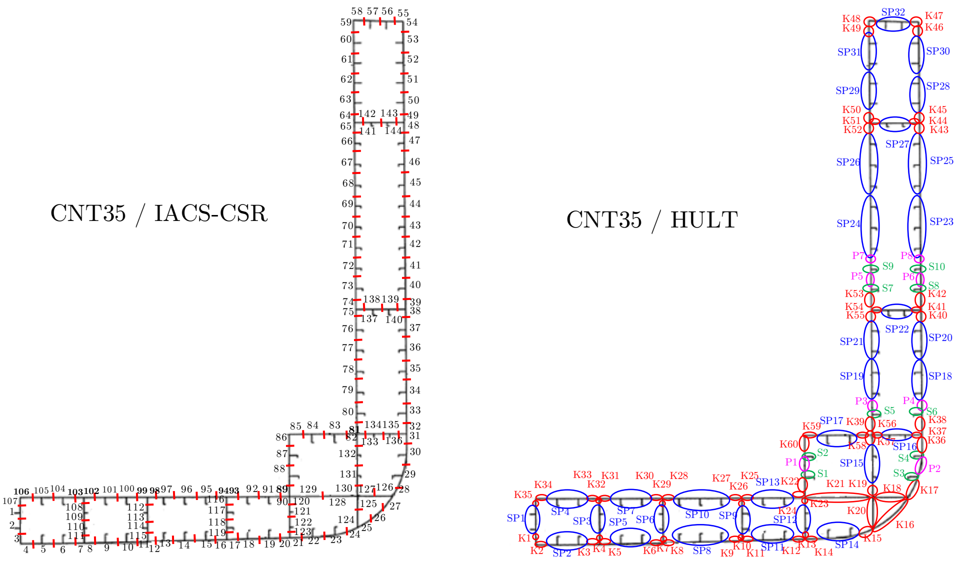

Figure 10: Two different component discretization of the mid-ship section.

After different component discretization, first of all, progressive collapse analysis are conducted by IACS-CSR and HULT in order to make comparison with results from literature. Average initial deflection and average residual welding strength values are preferred for components in progressive collapse analysis both hogging and sagging positions.

Comparative results with literature are given in Table 8. Next, considering Table 5, the progressive collapse calculations are repeated for different scenarios and comparative results (effects of initial deflections and residual welding strength) are represented in Figure 11.

		IACS-CSR	Chen	ALPS/HULL	FEM	Rina Rules	Rigo-2	Yao	HULT
(Sagging)	M_u x10^6 kN.m	6.81	5.47	6.64	6.95	5.89	6.91	6.72	6.68
	κ_u	1.65x10^{-4}	1.13x10^{-4}	1.5x10^{-4}	2.7x10^{-4}	2.09x10^{-4}	1.58x10^{-4}	1.41x10^{-4}	1.52x10^{-4}
(Hogging)	M_u x10^6 kN.m	6.65	6.56	6.92	6.97	6.86	7.20	6.72	6.83
	κ_u	1.94x10^{-4}	2.49x10^{-4}	1.87x10^{-4}	2.17x10^{-4}	2.49x10^{-4}	1.62x10^{-4}	1.63x10^{-4}	1.57x10^{-4}

Table 8: Moment and curvature values at ultimate strength of container ship (CNT35).

The values from literature in the table were digitized by related software programmes from graphs obtained in ISSC-2000 and ISSC-2012 benchmark studies. As seen from table, the results are well agreed with literature. Collapse strength results in hogging differs from 6.56 to 7.20 and can be accepted approximately close to each other. In sagging, results differs from 5.47 to 6.95 and can be accepted widely distributed. Two reasons can be said about this discrepancy in hogging and sagging results. First, mostly slender plate ratios of the components above the neutral axis that likely to Euler buckling collapse first in comparison with thick bottom components. Second, the local buckling strength of bottom panel components' is close to yield strength.

In the post-processing (results evaluation) part of the HULT, component by component collapse is able to be observed during progressive collapse calculations until hull girder section collapsed. For example, in sagging case, the calculation step that the vertical bending moment is 6.12x10^6 kNm and the curvature is 1.23 x10^{-3} 1/m, the upper deck plates and side plates were reached the local ultimate strength, firstly. Next, the calculation step that the vertical bending moment is 6.55x10^6 kNm and the curvature is 1.37x10^{-3} 1/m, the upper deck longitudinal stiffeners were reached the local ultimate strength. After that, the calculation step that the vertical bending moment is 6.63x10^6 kNm and the curvature is 1.43x10^{-3} 1/m, the second deck longitudinal stiffeners and side longitudinal stiffeners were reached the local ultimate strength. And the last, the calculation step that the vertical bending moment is 6.68x10^6 kNm and the curvature is 1.52x10^{-3} 1/m, the side plates between upper deck and second deck were collapsed and the hull girder section reached the global ultimate strength.

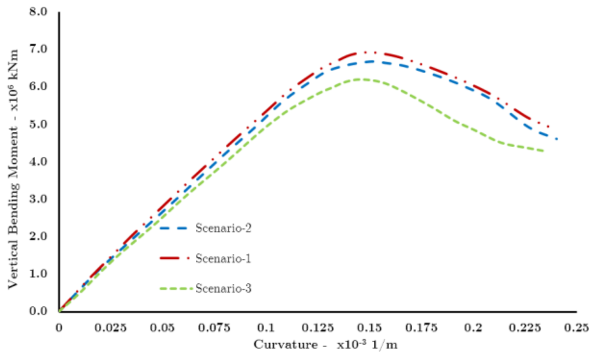

-a-

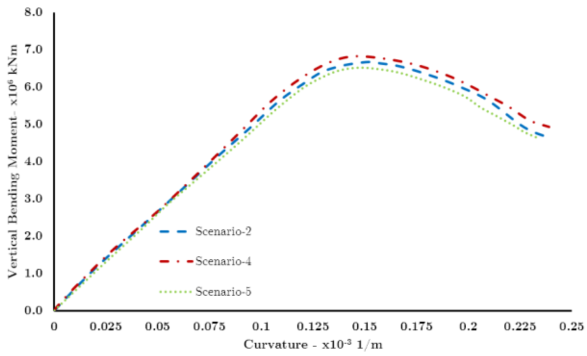

-b-

Figure 11: (a) Effect of initial deflections (b) Effect of residual welding strength on ultimate strength of hull girder.

According to the graphs given in Fig. 11, it can be observed that the effect of initial deflection is higher than effect of welding residual strength. There are clear decrease for collapse strength when initial deflection values increased while welding residual strength is constant. Given its strong influence, the initial deflections should be considered in progressive collapse analysis of ship hull girder.

This decrease effect can also be seen when welding residual strength is increased while initial deflection is constant. However, this effect has no significance to taken into account, so it can be neglected in calculations. In this case, welding residual strength have to be taken into account for a young new built (1-3 age) ship. Contrary, unless the ship have structural renovations, this effect can be neglected for 4+ aged ships, thinking that the effects of welding has gone.

4 CONCLUSIONS

In this paper, developed systematic calculation for hull girder ultimate strength analysis by authors, namely HULT is presented briefly and its reliability is tested by benchmark analysis for ten ships, firstly. The main target of the first part of this study is to bring out the reliability and applicability of progressive hull girder collapse calculations by HULT.

Next, HULT is used clearly representing the effect of hull section component discretization is tested by benchmark analysis for five different type ships. The main target of the second part of study is to bring out the effect of component discretization on progressive hull girder collapse calculations by HULT.

At the last part, the effects of initial distortions on progressive hull girder collapse calculations results by HULT is observed by using a typical double sided-double bottom container ship.

For all benchmark ships detailed analysis of collapse sequence for both hogging and sagging conditions are performed for all models. As expected, obtained ultimate strength (maximum load carrying capacity) values are higher for hogging than sagging for all calculations. The collapse of the compression flange of the tanker hulls takes place prior to the yielding of the tension flange as expected from usual ship hull girders. Thus, the ultimate hogging moment of the tanker hull is higher than the ultimate sagging moment as usual. It should also be emphasized for all models that decks which collapse first even for hogging case are the most critical and determinant portion of the hull girder transverse section.

Figure 7 compares the progressive collapse behavior of the ship hull under vertical bending moment, as obtained by the three type discretized models. It is observed that the results obtained from the various types of structural modelling considered are similar both hogging and sagging. Results of Model III for all ships are obtained nearly between and closer Model I and Model II results. In this regard, the simpler model (including small number component as possible as) extending between two adjacent transverse web frames may usually be appropriate for the progressive collapse analysis of ship's hulls. In this way, the less load-axial end shortening curve will be needed and this will decrease the computation time.

Results obtained by different methods and for different models were considered for calculation of Mean, St. Dv. and COV values of progressive collapse calculations. Coefficient of variation (COV) calculated for all methods and models are given in Table 4 for component discretization effects. COV for all methods varies from 0.021 to 0.101. Also, it can be observed that the results from Model I for all ships are close but have small differences from CSR-KTU results.

Last of all, according to the results of verification case studies, it can be observed that calculations with HULT and implementation of IACS-CSR method used by authors closely compatible with overall mean values for all benchmark ship hull girder models. Also, as a main consequence, developed calculation flow including stress-strain curves for single plate, stiffener and stiffened panel can be reliably merged to progressive hull girder collapse analysis with different component discretization in terms of the resulting approximations. Hereby, HULT has adequate reliability to estimate hull girder ultimate bending moment and determining the collapse sequence of structural components for all models.

Beside the good correlations among HULT and other results, the HULT should continue to be developed further taking into consideration some important effects such as transversely axial in plane loads, lateral out of plane loads (wave loads) and more realistic boundary conditions (elastically restrained edges) between plate-plate or plate-stiffener structural components.

References

Andric, J., Kitarovic, S., Bicak, M. (2014). IACS incremental - iterative method in progressive collapse analysis of various hull girder structures, Brodogradnja/Shıpbuıldıng 65/1: 65-78.

Benson, S. (2011). Progressive collapse assessment of lightweight ship structures, Ph.D. Thesis, Newcastle University, UK.

Caldwell, J. B. (1965). Ultimate longitudinal strength, Transactions RINA 107: 411-30.

Dalma, E. (2009). Ultimate hull girder strength assessment using semi-analytical and computational methods, PhD Thesis, National Technical University of Athens, Greece.

Dow, R. S. (1991). Testing and analysis of a 1/3 scale welded steel frigate model, Proc. Int. Conf. on Advances in Marine Structures, ARE, 749-773.

Hughes, O. and Paik, J. K. (2010). Ship Structural Analysis and Design, SNAME, New Jersey.

IACS-CSR (2012). International Association of Classification Societies, Common Structural Rules for Double Hull Oil Tankers and Bulk Carriers.

Marguerre, K. (1938). Zur theorie der gekrümmmter platte grosser formanderung proc. 5th Int. Congress Appl. Mech.93.

Ölmez, H. (2014). Ultimate strength estimation of ship hull girders by progressive collapse analysis approach, PhD Thesis, Karadeniz Technical University, Trabzon-Turkey.

Özgüç, Ö. (2006). Hull girder ultimate strength and fracture toughness of damaged marine structures, PhD Thesis, Universities of Glasgow and Strathclyde, UK.

Paik, J. K., Kim, B. J., Seo, J. K. (2008). Methods for ultimate limit state assessment of ships and ship-shaped offshore structures: part III-hull girders, Elsevier Science Direct Ocean Engineering 35: 281-286.

Paik, J. K., Wang, G., Kim, B. J., Thayamballi, A. K. (2002). Ultimate limit state design of ship hulls, SNAME Transactions 110: 85-114.

Paik, J.K., Hughes, O.F., Mansour, A.E. (2001). Advanced closed-form ultimate strength formulation for ships, Journal of Ship Research, 45/2: 111-32.

Rutherford, S.E. and Caldwell, J.B. (1990). Ultimate longitudinal strength of ships: a case study, SNAME Transactions. 98: 441-471.

Smith, C. S. (1976). Compressive strength of welded steel ship grillages, Transactions of the Royal Institution of Naval Architects 118: 325–359.

Smith, C. S. (1977). Influence of local compressive failure on ultimate longitudinal strength of a ship's hull, PRADS-International Symposium on Practical Design in Ship Building 73-79, Tokyo-Japan.

Smith, C. S., Davidson, P. C., Chapman, J. C., and Dowling, P. J. (1988). Strength and stiffness of ships' plating under in-plane compression and tension, RINA Transactions, 130: 277-296.

Smith, M. J. (2008). Ultimate strength assessment of naval and commercial ships. Defence R&D Canada – Technical Report DRDC Atlantic TR 2008-059.

Tayyar, G. T. (2011). Determination of ultimate strength of the ship girder, PhD Thesis, İstanbul Technical University, İstanbul-Turkey.

Technical Committee III.1. (2012). Ultimate strength, Proceedings of the 18th International Ship and Offshore Structures Congress, Rostock 1.

Technical Committee VI.2 (2000). Ultimate hull girder strength, Proceedings of the 14th International Ship and Offshore Structures Congress 2 Nagasaki.

Ueda, Y., Rashed, S. M. H. (1991). ISUM (Idealized Structural Unit Method) Applied to Marine Structures, Transactions of JWRI 20/1: 123-136.

URL-I (2013). http://www.vesselfinder.com/news/1223-UPDATE-MOL-Comfort-Sank,

Von Karman, T., Sechler, E. E., Donnell, L. H. (1932). Strength of thin plates in compression, ASME Trans, 54: 553-557.

Yao, T. (2003). Hull girder strength, Marine Structures 16: 1-13.